

Development of High-Performance Epoxy/Clay Nanocomposites by Incorporating Novel Phosphonium Modified Montmorillonite

Keiji Saitoh,^{1,2} Kenji Ohashi,¹ Toshiyuki Oyama,² Akio Takahashi,² Joji Kadota,³ Hiroshi Hirano,³ Kiichi Hasegawa³

¹ Hokko Chemical Industry Co. Ltd., 2165, Toda, Atsugi, Kanagawa 243-0023, Japan

² Faculty of Engineering, Yokohama National University 79-5, Tokiwadai, Hodogaya-ku, Yokohama, Kanagawa 240-8501, Japan

³ Osaka Municipal Technical Research Institute 1-6-50, Morinomiya, Joto-ku, Osaka 536-8553, Japan

Received 15 June 2010; accepted 7 September 2010

DOI 10.1002/app.33432

Published online 5 May 2011 in Wiley Online Library (wileyonlinelibrary.com).

ABSTRACT: Novel organoclays were synthesized by several kinds of phosphonium cations to improve the dispersibility in matrix resin of composites and accelerate the curing of matrix resin. The possibility of the application for epoxy/clay nanocomposites and the thermal, mechanical, and adhesive properties were investigated. Furthermore, the structures and morphologies of the epoxy/clay nanocomposites were evaluated by transmission electron microscopy. Consequently, the incorporation of organoclays with different types of phosphonium cations into the epoxy matrix led to different morphologies of the organoclay particles, and then the distribution changes of silicate layers in the epoxy resin influenced the physical properties of the nanocomposites. When high-reactive phospho-

nium cations with epoxy groups were adopted, the clay particles were well exfoliated and dispersed. The epoxy/clay nanocomposite realized the high glass-transition temperature (T_g) and low coefficient of thermal expansion (CTE) in comparison with those of neat epoxy resin. On the other hand, in the case of low-reactive phosphonium cations, the dispersion states of clay particles were intercalated but not exfoliated. The intercalated clay did not influence the T_g and CTE of the nanocomposite. © 2011 Wiley Periodicals, Inc. *J Appl Polym Sci* 122: 666–675, 2011

Key words: epoxy; nanocomposites; organoclay; curing behavior; exfoliation; thermal properties; adhesive properties

INTRODUCTION

Epoxy resins are widely used as adhesives, paints, laminates, coatings to electrical insulators, construction materials because of their superior thermal, mechanical, and electrical properties. However, making to higher performance is demanded in each field. For instance, the tendency of high performance, minitization and lightening in the electronic products are advancing. Especially, requirements of higher heat resistance and lower coefficient of thermal expansion (CTE) are severer than current performances in technical fields such as printed wiring board and plastic IC packages. As one of the solutions, the use of hybrid materials of polymers with inorganic materials at nano level is obviously attracts attention.^{1–4} Nanocomposite materials have been researched from both of academic and industrial viewpoints because they exhibit dramatic

improvement in properties even at very low filler contents. It has been regarded that this technology is applicable to the insulating material fields such as the low-k films, which cannot be filled up with much fillers.

The most popular clay used is based on the smectite class of aluminum silicate clays, of which the most common representative is montmorillonite (MMT). Generally, untreated clays are not applied for nanocomposites and it is necessary to prepare organoclays, which are incorporated organic cations via cation exchange reaction. Then, it becomes possible for nanocomposites to improve the affinity between the clay and polymer. In the field of thermosetting polymers, polymer/clay nanocomposites have been not yet industrialized. However, the improvement of various properties has been reported about the epoxy/clay nanocomposites by incorporating ammonium modified clay in many reports.^{5–23} For example, Kornmann et al. prepared the epoxy resins filled with various amine modifiers and showed the morphologies and thermal, mechanical properties influenced with the addition of amine modifiers on the organoclays. They reported

Correspondence to: K. Saitoh (saitoh-kei@hokkochem.co.jp).

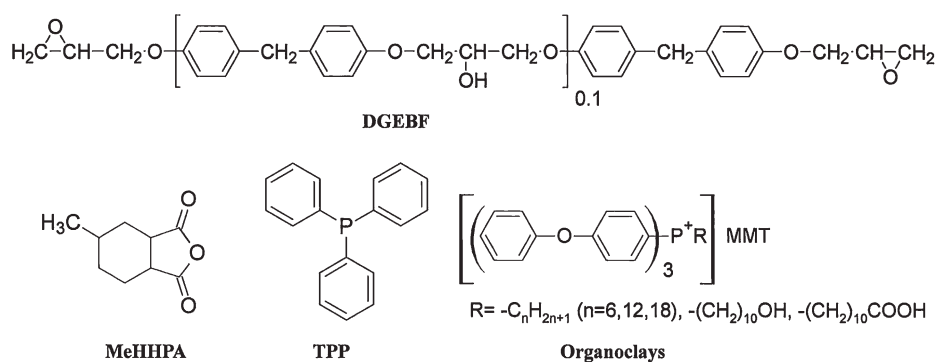


Figure 1 Chemical structures of materials used in this study.

the enhancements of flexural modulus and fracture properties on nanocomposites.^{22–24} However, in such nanocomposites, the reductions of desired heat resistance in aforementioned industry were reported.^{1,21,22} Therefore, it is necessary to improve the dispersibility of clay particles and to make effective design on the organic molecules of organoclays. As one of the means, it is important not to drop the thermal resistance and dispersibility of organoclays on condition of high-temperature by using high heat-resistant phosphonium modified MMT in comparison with ammonium modified MMT.

On the other hand, phosphine and phosphonium salt are used as a catalyst in organic synthesis and an epoxy curing accelerator in semiconductor molding compounds. These phosphine compounds have less soluble in water and high electric reliability than ammonium compounds. Furthermore, these phosphine compounds are superior to the corresponding ammonium compounds. Phosphonium modified MMT is expected to the applications of high-heat resistance filler and the latent epoxy curing accelerator. Also, epoxy/clay nanocomposite obtained by incorporating phosphonium modified clay is available to electronic materials, which are desired the properties of heat resistance, flammability, and low CTE. However, only few attempts have been made so far to use the phosphonium compounds as the organic modifiers, though it is possible for the organic modification to exchange with cations in same cases like ammonium compounds.^{24,25} Although the improvements in the flammability and mechanical property have been investigated in these epoxy/clay nanocomposites, how to restrain the reduction of thermal resistance is as a problem for epoxy/clay nanocomposites as well as ammonium systems. In our previous paper, organo-bentonites introduced with novel quaternary phosphonium salt were prepared and investigated the developments for nanocomposites, and the effect on the properties of epoxy/clay nanocomposites was reported.²⁶

In this article, to research the influence on the dispersibility and characteristics in epoxy/clay nanocomposites, the previous works are more pushed ahead. Specifically, we designed and prepared various organoclays modified with different functional groups, which have both compatibility with epoxy resins and ability for the curing accelerator, due to enhance the affinity with epoxy/clay nanocomposite in this research. The dispersibility and the influence on the properties of epoxy/clay nanocomposites are presented.

EXPERIMENTAL

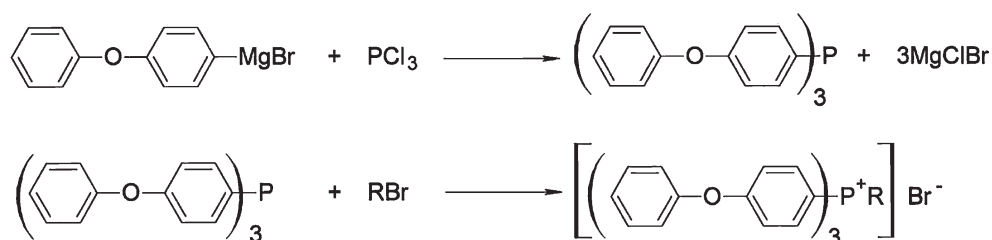
Materials

4-Bromodiphenylether, 1-bromohexane, 1-bromododecane, 1-bromooctadecane, 11-bromoundeca acid, and 10-bromo-1-decanol were purchased from Tokyo Chemical Industry Co. Phosphorus trichloride (PCl_3), which was purchased from Kanto Chemical Co., was used without any purification. The solvents used in this work were commercially available and used as received.

The epoxy resin used was diglycidyl ether of bisphenol-F (DGEBF, jER807, Japan Epoxy Resins Co.), which had an epoxide equivalent weight of 170 g/equiv. 4-Methyl hexahydrophthalic anhydride (MeHHPA, RIKACID MH-700G, New Japan Chemical Co.) was used as the curing agent. The unmodified clay used in this study was a natural MMT (BEN-GEL A) supplied from Hojun Co. Triphenylphosphine (TPP) obtained from Hokko Chemical Industry Co. was used as the curing accelerator for neat epoxy resin. Figure 1 shows the structures of the materials used in this study.

Synthesis of various quaternary phosphonium salts

Tris(4-phenoxyphenyl)phosphine was synthesized from 4-bromodiphenylether and PCl_3 by the Grignard reaction. This phosphine was a whitish to slightly yellowish powder; m.p. 110–112°C. 10-



Scheme 1 Synthesis of different quaternary phosphonium salts.

Carboxydecyltris(4-phenoxyphenyl)phosphonium bromide was prepared as reported in a previous study.²⁶ Furthermore, 10-hydroxydecyltris(4-phenoxyphenyl)phosphonium bromide, hexyltris(4-phenoxyphenyl)phosphonium bromide, dodecyltris(4-phenoxyphenyl)phosphonium bromide, and octadecyltris(4-phenoxyphenyl)phosphonium bromide in this study were synthesized by the procedure shown in Scheme 1. These phosphonium salts were obtained as pale orange-colored semisolid. ¹H- and ³¹P-NMR experiments in solutions were individually performed on a JEOL NMR spectrometer. Infrared spectra were recorded on a FTIR spectrometer using KBr pellets. Figures 2 and 3 show ¹H-NMR spectrum and IR spectrum, respectively, for 10-hydroxydecyltris(4-phenoxyphenyl)phosphonium bromide.

10-Carboxydecyltris(4-phenoxyphenyl)phosphonium bromide

Yield 92.5%, pale orange-colored semisolid. ¹H-NMR (300 MHz, CD₃OD, TMS basis) δ (ppm): 7.71–

7.79 (m, 6H, Ar-H), 7.40–7.47 (m, 6H, Ar-H), 7.09–7.29 (m, 15H, Ar-H), 3.29–3.34 (2H, P-CH₂-), 2.21–2.26 (2H, CH₂-COOH), 1.55–1.60 (6H, -CH₂-), 1.27 (10H, -CH₂-). ³¹P-NMR (300 MHz, CD₃OD, H₃PO₄ basis) δ (ppm): 23.0. IR (KBr, cm⁻¹): 3350 (νOH, COOH), 2928, 2855 (νC-H), 1732 (νC=O), 1582, 1487 (νC=C, Ar), 1250 (νC-O-C, Ar).

10-Hydroxydecyltris(4-phenoxyphenyl)phosphonium bromide

Yield 78.1%, pale orange-colored semisolid. ¹H-NMR (300 MHz, CD₃OD, TMS basis) δ (ppm): 7.71–7.78 (m, 6H, Ar-H), 7.42–7.48 (m, 6H, Ar-H), 7.11–7.30 (m, 15H, Ar-H), 3.29–3.39 (m, 4H, P-CH₂-, -CH₂OH), 1.52–1.62 (m, 6H, -CH₂-), 1.29 (m, 10H, -CH₂-). ³¹P-NMR (300 MHz, CD₃OD, H₃PO₄ basis) δ (ppm): 23.2. IR (KBr, cm⁻¹): 3323 (νOH, OH), 3059, 3038, 3011 (νC-H, Ar), 2928, 2860 (νC-H, Alkyl), 1582, 1487 (νC=C, Ar), 1252 (νC-O-C, Ar).

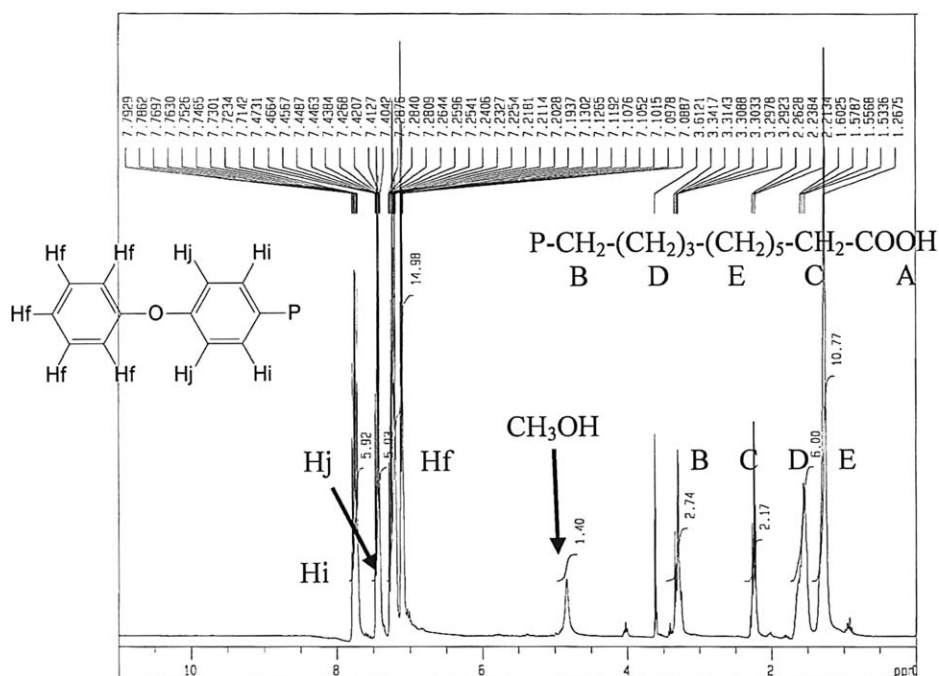


Figure 2 ¹H-NMR spectrum of 10-carboxydecyltris(4-phenoxyphenyl)phosphonium bromide (CD₃OD).

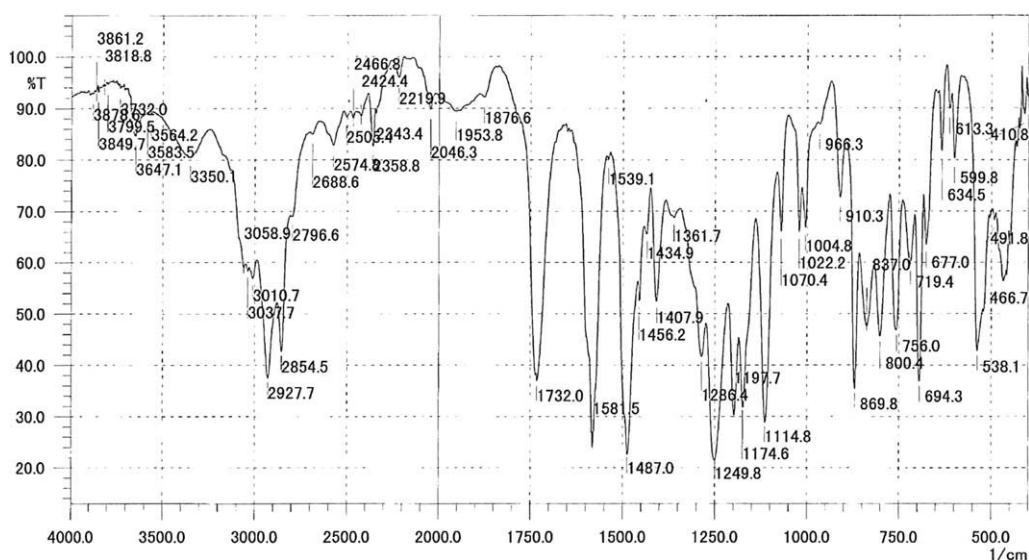


Figure 3 IR spectrum of 10-carboxydecyltris(4-phenoxyphenyl)phosphonium bromide (KBr disk).

Hexyltris(4-phenoxyphenyl)phosphonium bromide

Yield 47.1%, pale orange-colored semisolid. $^1\text{H-NMR}$ (300 MHz, CD_3OD , TMS basis) δ (ppm): 7.70–7.78 (m, 6H, Ar-H), 7.42–7.48 (m, 6H, Ar-H), 7.11–7.30 (m, 15H, Ar-H), 3.29–3.31 (m, 2H, P- CH_2 -), 1.52–1.60 (m, 4H, - CH_2 -), 1.28–1.30 (m, 4H, - CH_2 -), 0.87–0.89 (m, 3H, - CH_3). $^{31}\text{P-NMR}$ (300 MHz, CD_3OD , H_3PO_4 basis) δ (ppm): 23.0. IR (KBr, cm^{-1}): 3059, 3038, 3011 ($\nu\text{C-H}$, Ar), 2955, 2930, 2860 ($\nu\text{C-H}$, Alkyl), 1582, 1487 ($\nu\text{C=C}$, Ar), 1252 ($\nu\text{C-O-C}$, Ar).

Dodecyltris(4-phenoxyphenyl)phosphonium bromide

Yield 77.4%, pale orange-colored semisolid. $^1\text{H-NMR}$ (300 MHz, CD_3OD , TMS basis) δ (ppm): 7.69–7.77 (m, 6H, Ar-H), 7.43–7.49 (m, 6H, Ar-H), 7.11–7.30 (m, 15H, Ar-H), 3.29–3.31 (m, 2H, P- CH_2 -), 1.52–1.60 (m, 4H, - CH_2 -), 1.26–1.28 (m, 16H, - CH_2 -), 0.86–0.89 (m, 3H, - CH_3). $^{31}\text{P-NMR}$ (300 MHz, CD_3OD , H_3PO_4 basis) δ (ppm): 23.2. IR (KBr, cm^{-1}): 3059, 3040, 3011 ($\nu\text{C-H}$, Ar), 2924, 2853 ($\nu\text{C-H}$, Alkyl), 1582, 1487 ($\nu\text{C=C}$, Ar), 1252 ($\nu\text{C-O-C}$, Ar).

Octadecyltris(4-phenoxyphenyl)phosphonium bromide

Yield 81.4%, pale orange-colored semisolid. $^1\text{H-NMR}$ (300 MHz, CD_3OD , TMS basis) δ (ppm): 7.68–7.76 (m, 6H, Ar-H), 7.36–7.43 (m, 6H, Ar-H), 7.03–7.24 (m, 15H, Ar-H), 3.25–3.30 (m, 2H, P- CH_2 -), 1.50–1.53 (m, 4H, - CH_2 -), 1.22 (m, 28H, - CH_2 -), 0.81–0.86 (m, 3H, - CH_3). $^{31}\text{P-NMR}$ (300 MHz, CD_3OD , H_3PO_4 basis) δ (ppm): 23.2. IR (KBr, cm^{-1}): 3059, 3040, 3011 ($\nu\text{C-H}$, Ar), 2924, 2853 ($\nu\text{C-H}$, Alkyl), 1582, 1487 ($\nu\text{C=C}$, Ar), 1250 ($\nu\text{C-O-C}$, Ar).

Preparation of organoclays

Na-MMT (BEN-GEL A, Hojun Co.) has a cation exchange capacity (CEC) value of 93.9 mmol/g. Na-MMT (21.6 g, 0.02 mol) was added to water (1000 g) with rapid stirring to prepare the 2 wt % aqueous dispersion of MMT. 10-Carboxydecyltris-(4-phenoxyphenyl)-phosphonium bromide (19.3 g, 0.024 mol) was dissolved in 200 mL of methanol and poured into the 2 wt % aqueous dispersion of the pristine clay. The mixture was vigorously stirred for 3 h at 50°C. The reaction mixture was filtered and washed with methanol and water, and then freeze-dried in a vacuum. The dried product was ground and sieved to a particle size <250 μm (C_{10}CM). By the same preparation method, C_{10}HM , C_6AM , C_{12}AM , and C_{18}AM were prepared, respectively. These organoclays are listed in Table I.

Preparation of epoxy/clay nanocomposites

An appropriate amount of organoclay was added to 100 g of DGEBF, and the mixture was stirred. MeHHPA (85.3 g) was added to the mixture and stirred, and then followed by ultrasonic mixing with an ultrasonic homogenizer. The resulting mixtures were poured into a mold and cured at 120°C for 3 h, and then post-cured at 160°C for 6 h. Each epoxy nanocomposite incorporated with each organic modifier (5 wt % or 7 wt % silicate loading) was prepared to investigate the physical properties of the epoxy nanocomposites. The composition ratio of the epoxy/clay nanocomposites was shown in Table II. Epoxy resin/curing agent ratio was maintained at 100 : 85.3 (DGEBF/hardener) by weight in all samples prepared. Because the hydroxyl or carboxyl group of phosphonium modified MMT could react

TABLE I
Composition of Matrix Resins

Abbreviation	Clay	Cations	d-spacing (Å)	Organic content (%)
M	MMT	–	11.8	–
C ₆ AM	C ₆ -MMT	R ₃ P ⁺ C ₆ H ₁₃	20.3	27.6
C ₁₂ AM	C ₁₂ -MMT	R ₃ P ⁺ C ₁₂ H ₂₅	23.0	31.2
C ₁₈ AM	C ₁₈ -MMT	R ₃ P ⁺ C ₁₈ H ₃₇	24.6	35.4
C ₁₀ HM	C ₁₀ OH-MMT	R ₃ P ⁺ (CH ₂) ₁₀ OH	21.8	31.3
C ₁₀ CM	C ₁₀ COOH-MMT	R ₃ P ⁺ (CH ₂) ₁₀ COOH	22.4	34.4

with DGEBF, the curing agent was reduced against DGEBF. As a reference, neat epoxy resin was obtained by the same curing condition without the addition of clay.

Characterization

NMR spectra were recorded on a JEOL JNM-LAMBDA 300 spectrometer. Fourier transform infrared (FTIR) spectra were measured for specimens pressed in KBr tablets on a Shimadzu model FTIR-8300. X-ray diffraction (XRD) analysis was performed on the RINT ULTIMA (Rigaku Corporation) with Cu radiation (40 kV, 20 mA). Swelling power was measured by following method; 2 g of the samples were poured into 100 mL of acetone in mass cylinder. After 24 h, the apparent volume (mL/2 g) of the swelling clay was measured according to JBAS-104-77. Thermogravimetric analysis (TGA) was conducted using a Bruker model TG-DTA 2000S, by heating the samples from room temperature to 800°C at a rate of 10°C/min under air. Curing behaviors of epoxy/clay mixtures were studied using a differential scanning calorimeter (DSC) on a Bruker model DSC 3100S at a heating rate of 10°C/min between 25°C and 300°C. Transmission electron micrographs (TEM) were taken with a JEM-2000FXII apparatus at an acceleration voltage of 100 kV. Dynamic mechanical analysis (DMA) was performed on a dynamical mechanical analyzer SDM5600 DMS110 in the three-point bending mode at a frequency of 1 Hz over the temperature range 25–250°C. The heating rate was 2°C/min. The dynamic

storage modulus (E') and $\tan \delta$ against temperature curves were recorded and plotted. The temperature at which the $\tan \delta$ curve shows a maximum peak is recorded as the glass transition temperature (T_g). The CTE was measured using a thermo mechanical analyzer (TMA/SS6100, SII Nanotechnology) by recording in dimension of the specimens with temperature. The specimens, in cubic form ($4 \times 4 \times 10 \text{ mm}^3$), were heated from 25°C to 250°C at a rate of 2°C/min. The CTE value was calculated between 50°C and 100°C. Tensile test was carried out according to JIS K6851. It was measured by using Universal Testing Machine (AI-50kNB, Minebea Co.) at a speed of 5 mm/min.

RESULTS AND DISCUSSION

Characterization of organoclays

Figure 4 shows the XRD patterns of pristine clay and several different kinds of organoclay. Their d-spacings were calculated by use of Bragg's relation according to the angle of the 001 diffraction peaks in the XRD patterns. The all observed shifts of diffraction peaks to smaller angles in comparison with pristine clay mean stretches of distances between the silicate layers of the organoclays. For example, the d-spacing for C₁₀HM and C₁₀CM are 21.8 and 22.4 Å, respectively, compared with the

TABLE II
Composition of Nanocomposites

Epoxy/hardener/ clay/content	DGEBF	MH700	Organoclay	TPP
Control with TPP	100	85.3	–	0.94
EP/MH700/C ₆ AM/5	100	85.3	9.8	–
EP/MH700/C ₁₂ AM/5	100	85.3	9.8	–
EP/MH700/C ₁₈ AM/5	100	85.3	9.8	–
EP/MH700/C ₁₀ HM/5	100	85.3	9.8	–
EP/MH700/C ₁₀ CM/5	100	85.3	9.8	–
EP/MH700/C ₁₀ CM/7	100	85.3	14.0	–

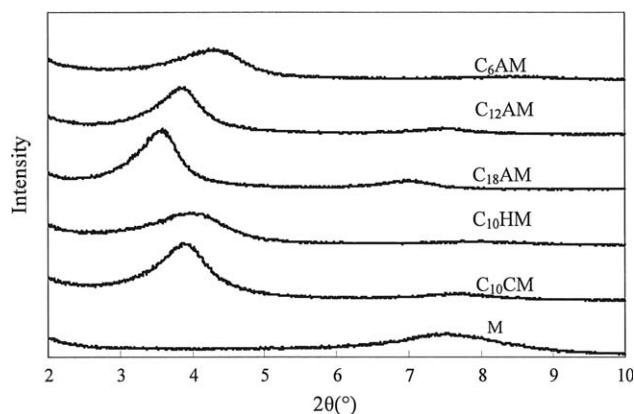


Figure 4 XRD patterns of non modified clay and various organoclays.

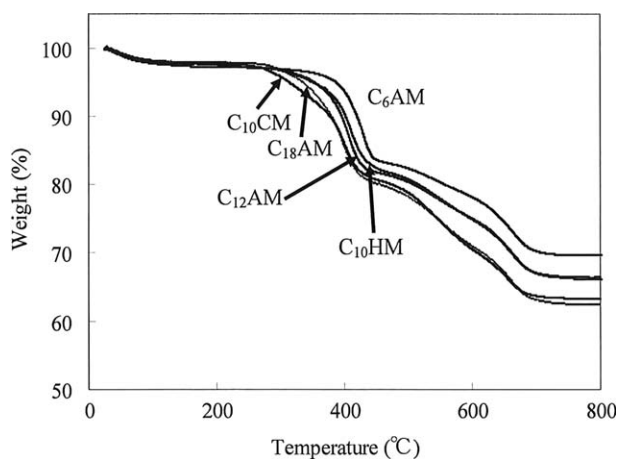


Figure 5 Thermal stability of the different organoclays evaluated using thermogravimetric analysis under air.

original d-spacing of MMT, 11.8 Å. The d-spacing of the organoclays having substituted long alkyl chain were found to be 20.3, 23.0, and 24.6 Å for C₆AM, C₁₂AM, and C₁₈AM, respectively. This indicates that the interlayer spacing becomes wider as the chain length of organo-surfactant increases on the organic modifier. TGA measurements were applied to evaluate the organic modifier contents of organoclays. The various TGA thermograms of organoclays containing different phosphonium cations under air are presented in Figure 5. As shown in Figure 5 and Table I, the organic contents of organoclay were calculated at the temperature range of 200–800°C, which were related to the thermal decomposition of the organo-surfactants. Consequently, as the molecular weight of organo-surfactants increased, the organic weight con-

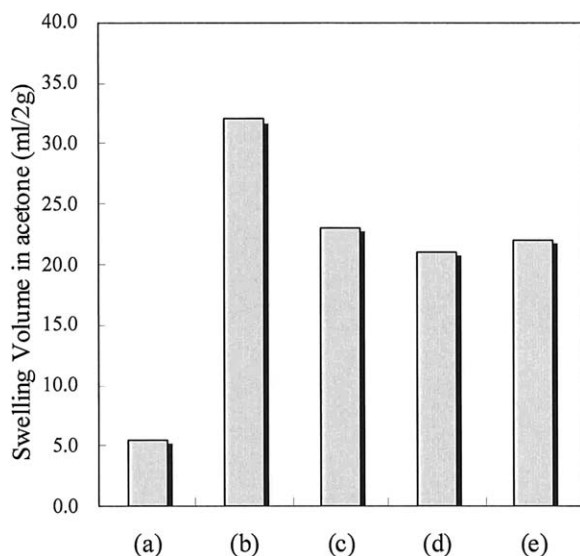


Figure 6 Swelling volume in acetone for the different organoclays, (a) Pristine clay (M), (b) C₁₀CM, (c) C₁₀HM, (d) C₁₂AM, and (e) C₁₈AM.

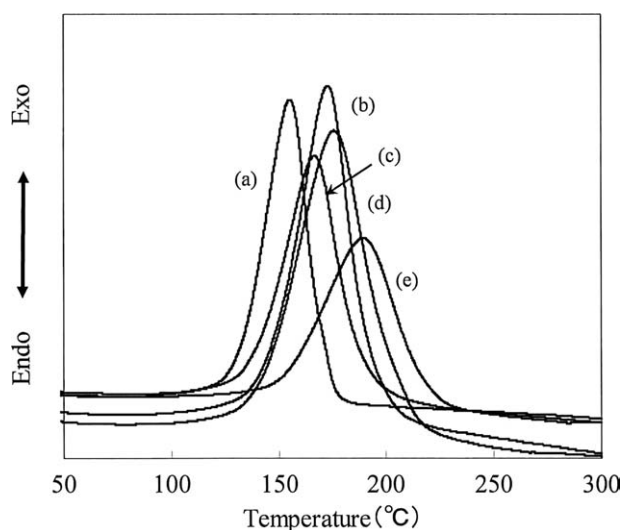


Figure 7 DSC curves of the control epoxy added TPP (a) and epoxy/clay mixtures containing, (b) C₁₀CM/5, (c) C₁₀CM/7, (d) C₁₈AM/5, and (e) C₁₀HM/5.

tents of organoclay increased. For C₆AM, it has better thermal stability than C₁₀CM and C₁₈AM. This can be attributed to sensitiveness against the heat on the long alkyl chains of C₁₀CM and C₁₈AM.

Moreover, swelling power of unmodified MMT and some organoclays were measured in acetone to evaluate dispersibility of the polarity solvent. Swelling power of unmodified MMT was 5.5 mL/2 g, and it was hardly swelled in acetone. This indicates that epoxy/hardener mixture cannot penetrate into the gallery due to low swelling power. The presence of phosphonium cations in the gallery encourages the penetration of epoxy into the clay galleries leading to the formation of epoxy/clay nanocomposite.²³ The swelling power of C₁₀CM was 32.0 mL/2 g because of increase the interlayer distance for penetrating of acetone as shown in Figure 6. This implies that terminal carboxyl and phenoxyphenyl groups in C₁₀CM were compatibilized with acetone, and then swelling power was enhanced due to enter into the interlayers. On the other hand, swelling power of C₁₈AM was 22.0 mL/2 g and lower in comparison with that of C₁₀CM, though the d-spacing of C₁₈AM was expanded. This implies that the organoclay introduced alkyl phosphonium cation could not lead to enhance swelling power due to low compatibility with polar solvent as acetone.

Curing behaviors

To investigate the curing behaviors of epoxy/clay mixtures before curing, DSC was measured (Fig. 7). The control epoxy contained TPP shows a single exothermic peak at 155.5°C. In comparison with epoxy/nonclay mixture, the higher temperature peaks are observed at curing peaks of epoxy/clay mixtures

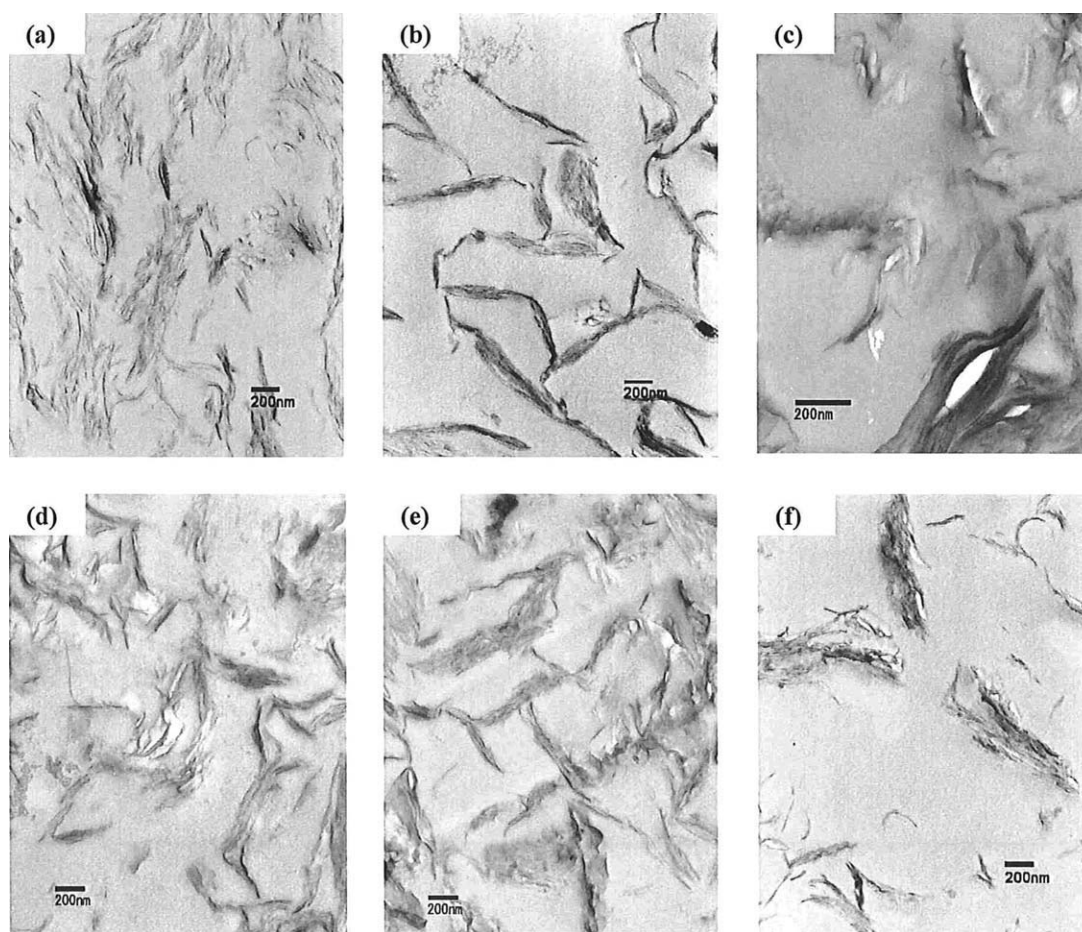


Figure 8 TEM images of epoxy/clay nanocomposites containing, (a) $C_{10}CM/5$, (b) $C_{10}CM/7$, (c) $C_{10}HM/5$, (d) $C_6AM/5$, (e) $C_{12}AM/5$ and (f) $C_{18}AM/5$.

with 5 wt % organoclays and 7 wt % organoclays. The peak temperature shifted to a lower temperature region with increasing $C_{10}CM$ content: 173.1°C for 5 wt % and 166.8°C for 7 wt %, respectively. This is considered that epoxy resin and acid anhydride could easily penetrate into the clay galleries and the epoxy curing reaction could proceed because the d-spacing of $C_{10}CM$ is broaden and $C_{10}CM$ has terminal COOH substituent. Furthermore, the maximum exothermic temperature shifts to lower temperature with increasing the clay content, and then it is found that incorporating various amounts of the organoclays into epoxy resin could control the curing temperature. Similarly, the curing reactions with epoxy resins and other organoclays were confirmed. These curing rates might be dependent on the organic contents of the organoclays. In such a way, the effect as an accelerator was confirmed in each case for $C_{10}CM$, $C_{10}HM$, C_6AM , $C_{12}AM$, and $C_{18}AM$.

Morphology of nanocomposites

The structure and morphology of the clay dispersion in nanocomposites were determined by TEM. The

TEM micrographs of epoxy/clay nanocomposites containing 5 wt % and 7 wt % of $C_{10}CM$ are shown in Figure 8(a,b), respectively. The exfoliated and homogeneously dispersed silicate layers in the acid anhydride-cured epoxy nanocomposites were observed. This indicates that the improvement of dispersion of silicate layers is believed to be because of the presence of the carboxyl group in quaternary phosphonium cation. The exfoliation mechanisms are proposed as follows. First, the penetration of DGEBF and acid anhydride between clay layers had taken place. The curing reaction started from the inside clay interlayer or the neighborhood, and hence, the individual silicate nanolayers were distorted and homogeneously and randomly dispersed throughout the epoxy matrix.^{21,23} Zilg et al. proposed that incorporation of reactive groups such as carboxyl or hydroxy group appeared to give only slightly improved interlayer separation.¹ On the other hand, the aggregated clay platelets of $C_{18}AM$ in epoxy/clay nanocomposite were observed in Figure 8(f). When compared with EP/MH700/ $C_{10}CM/5$, EP/MH700/ $C_{12}AM/5$ and EP/MH700/ $C_{18}AM/5$ showed more intercalated structures. This

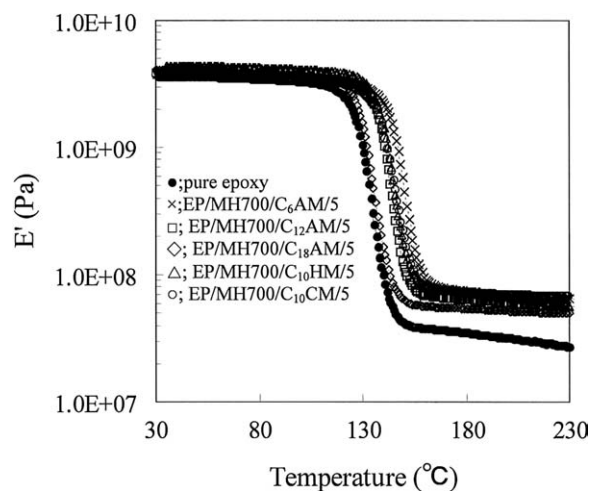


Figure 9 Temperature dependence of storage modulus (E') for epoxy/clay nanocomposites incorporated 5 wt % organoclays.

indicates that the presence of hydrophobic alkyl group and the lack of compatibility with the organoclay and the epoxy matrix could prevent the penetration of DGEBA and acid anhydride. These results agree with the results of swelling power. In the preparation of epoxy/clay nanocomposites, clay exfoliation is influenced by many factors, including curing agents and conditions, and the property of clay modifier.²³ The dispersion state of clay particles in the epoxy matrix resulted in different morphology. It was found that the formation of exfoliated clay nanocomposites could be dependent on the nature of the organoclay introduced with quaternary phosphonium cation.

Thermal characterization of nanocomposites

Thermal and thermal mechanical properties of the acid anhydride-cured epoxy nanocomposites were evaluated by DMA and TMA, respectively. The tem-

perature dependencies of the storage modulus of epoxy/clay nanocomposites filled with different organoclay loadings are shown in Figure 9. The physical properties of epoxy/clay nanocomposites are listed in Table III. The storage moduli in the rubbery region for epoxy/clay nanocomposites are high in comparison with the neat epoxy. Moreover, the storage moduli of epoxy/clay nanocomposites by incorporating alkyl-phosphonium modified MMT were lower than those of nanocomposites introduced with carboxyl-phosphonium modified MMT. This might indicate that the improvement of storage modulus in EP/MH700/C₁₀CM nanocomposite is attributed to the good dispersion of silicate layers, which restrict the mobility of polymer chains under loading as well as to the good interfacial adhesion between the silicate layers and the epoxy matrix. However, mobility of polymer chains could not be restricted due to the aggregation of clay particles in nanocomposite by incorporating alkyl-phosphonium modified MMT, and consequently storage modulus of nanocomposite could be low. The temperature dependencies of the $\tan \delta$ of epoxy/clay nanocomposites are shown in Figure 10. The T_g of neat epoxy resin observed at 138.1°C, whereas the T_g of epoxy/clay nanocomposites was observed at 150.4°C and 152.4°C for EP/MH700/C₁₀CM/5 and EP/MH700/C₁₀CM/7, respectively. This indicates that layered silicates in the epoxy matrix act as pseudo cross-linking points because of the interaction with the carboxyl group in quaternary phosphonium cation and the hydroxyl group of the clay. Interfacial adhesion of the silicate layers results predominantly from adsorption and can be enhanced by covalent coupling with functional groups.^{1,8} Hence, it can be considered that the good dispersion of silicate layers could lead to the increase of T_g to restrict the mobility of polymer chains. On the other hand, T_g of EP/MH700/C₁₈AM/5 increased slightly. This is attributed that the long alkyl chain of organo-surfactant

TABLE III
Physical Properties of Epoxy/Clay Nanocomposites

Epoxy/clay materials	Clay content (wt %)	DSC ^a			DMA ^b		TMA ^b
		T_{onset} (°C)	T_{peak} (°C)	T_g (°C)	E' (35 °C, MPa)	E' (T_g+40 °C, MPa)	CTE (ppm/K)
Control with TPP	0	132.0	155.5	138.1	3640	35.3	61.1
EP/MH700/C ₁₀ CM	5	143.1	173.1	150.4	3882	71.2	56.8
EP/MH700/C ₁₀ CM	7	136.7	166.8	152.4	4286	87.2	53.0
EP/MH700/C ₁₀ HM	5	152.7	189.3	148.1	4385	69.6	60.4
EP/MH700/C ₆ AM	5	152.3	203.5	152.4	3784	70.7	63.7
EP/MH700/C ₁₂ AM	5	142.9	183.7	146.7	3855	62.4	63.5
EP/MH700/C ₁₈ AM	5	141.4	176.0	140.8	4096	54.2	61.2

^a Epoxy/clay mixtures were measured by heating at the rate of 10°C/min.

^b Cured epoxy materials were measured.

in the organoclay could have the plasticity effect.^{2,22} When the length of the alkyl chain of surfactant is shortened, T_g of the EP/MH700 systems increases to reduce the plasticity effect of the alkyl chain on the organic surfactants. It can be suggested that organoclay with short alkyl chains leads to good dispersion of silicate layers. Zilg et al. reported that the T_g was influenced by incorporating silicate layers modified with different amine modifier.¹

The CTE of pure epoxy was 61.1 ppm/K. The CTE of EP/MH700/C₁₀CM/7 was 53.0 ppm/K, which is about 14% lower than that of neat epoxy resin. It was found that at a relatively low concentration led to the improvement of thermal mechanical properties in epoxy/clay nanocomposites. This is explained that the interfacial area of the well-dispersed silicate layers increases and restricts the thermal expansion of nanocomposite. Similarly, the CTE of EP/MH700/C₁₀HM was lower than that of the unmodified resin. Incorporations of the organoclays filled with high reactive carboxyl or hydroxyl groups would cause reduction of the CTE values in epoxy/clay nanocomposites. On the other hand, the CTE of epoxy/clay nanocomposites by incorporating alkyl phosphonium modified MMT did not change in comparison with that of neat epoxy resin. It thus indicates that the epoxy network may not be affected by the addition of organoclay introduced alkyl phosphonium cation.

Adhesive properties of nanocomposites

The results of tensile shear adhesive test are shown in Figure 11. All of samples showed cohesive failure and part interface failure. The tensile shear adhesive strength of nanocomposites by incorporating alkyl-

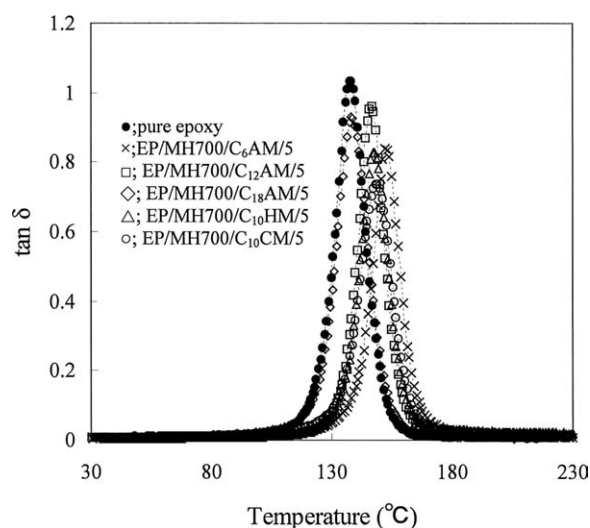


Figure 10 Temperature dependence of loss tangent ($\tan \delta$) for epoxy/clay nanocomposites incorporated 5 wt % organoclays.

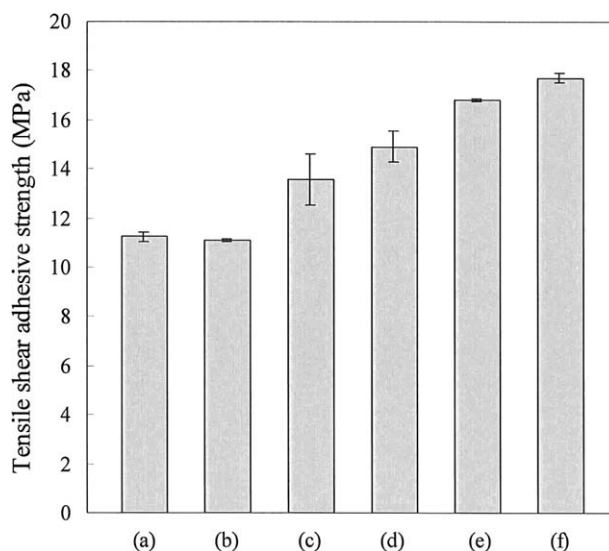


Figure 11 The results of tensile shear adhesive strength with neat epoxy (a) and epoxy/clay nanocomposites containing, (b) C₁₀CM, (c) C₁₀HM, (d) C₆AM, (e) C₁₂AM and (f) C₁₈AM.

phosphonium modified MMT increased in comparison with that of neat epoxy resin. Particularly, the adhesive strength of EP/MH700/C₁₈AM increased by 1.57 times compared with the neat epoxy resin. Silicate layers could not bridge with epoxy in nanocomposites by incorporating alkyl-phosphonium modified MMT which were not react with epoxy, and consequently, the tensile shear adhesive strength of nanocomposite could be enhanced due to increase stress relaxation. Furthermore, as lengthening the alkyl chains in phosphonium cation, the adhesive strength of nanocomposites can be improved to make stress relaxation possible. On the other hand, no difference was observed in the tensile shear adhesive strength of EP/MH700/C₁₀CM compared with that of neat epoxy resin. The exfoliated and homogeneously dispersed silicate layers in nanocomposite by incorporating carboxyl-phosphonium modified MMT could make homogeneously hard network in whole nanocomposite. Then, the tensile shear adhesive strength of nanocomposite might be reduced to decrease stress relaxation.

CONCLUSIONS

The epoxy/clay nanocomposites have been extensively studied to achieve the enhancement in the flammability and mechanical properties. On this occasion, the treatments of the pristine clay with the organic modifiers are essential, but all sorts of accompanying the reduction in thermal resistance become important problems. We have studied the epoxy/clay nanocomposites by incorporating phosphonium modified MMT due to solve these

problems. In this work, we designed and prepared various organoclays, which have both compatibility with epoxy resins and ability for the curing accelerator, due to improve the thermal resistance, the mechanical properties, and the adhesion on epoxy/clay nanocomposite. Then, we investigated to apply to epoxy/clay nanocomposite. Consequently, we found that the organic modifiers of organoclays influenced various properties on epoxy/clay nanocomposites. First, the TEM observations of nanocomposite by incorporating carboxyl-phosphonium modified MMT showed that silicate layers were well exfoliated and dispersed in the epoxy matrix. Besides, the high T_g and low CTE of nanocomposites were observed in comparison with those of neat epoxy resin. These results imply that carboxyl group can act as a curing accelerator or a cross linker as expected. On the other hand, the clay agglomerations in the morphology of epoxy/clay nanocomposites filled with alkyl-phosphonium modified MMT were revealed by TEM. The almost unchanged CTE values of nanocomposite filled with alkyl-phosphonium modified MMT were found to be in comparison with that of neat epoxy resin. As lengthening the alkyl chains in phosphonium cation, the tensile shear adhesive strengths of nanocomposites have been increased significantly. However, lengthening the alkyl chain length, T_g of these nanocomposites decreases due to the plasticity effect of the alkyl chain on organic surfactants.

From the above, it is confirmed that the dispersibility is improved in epoxy/clay nanocomposites by incorporating carboxyl-phosphonium modified MMT. As a result, obtained high-performance materials had exceptional thermal and thermal mechanical properties. On basis of these results, the developments of reforming materials for the epoxy resin are now planning.

We thank the Yokohama National University, Instrumental Analysis Center for help in conducting transmission electron microscopic analysis.

References

1. Zilg, C.; Mülhaupt, R.; Finter, J. *Macromol Chem Phys* 1999, 200, 661.
2. Lee, J. Y.; Lee, H. K. *Mater Chem Phys* 2004, 85, 410.
3. Hsu, S. L.-C.; Wang, U.; King, J.-S.; Jeng, J.-L. *Polymer* 2003, 44, 5533.
4. Yeh, J.-M.; Chang, K.-C. *J Ind Eng Chem* 2008, 14, 275.
5. Park, J.; Jana, S. C. *Macromolecules* 2003, 36, 2758.
6. Park, J.; Jana, S. C. *Macromolecules* 2003, 36, 8391.
7. Wang, M. S.; Pinnavaia, T. J. *Chem Mater Sci* 1994, 6, 468.
8. Shi, H.; Lan, T.; Pinnavaia, T. J. *Chem Mater Sci* 1996, 8, 1584.
9. Tagami, N.; Okada, M.; Hirai, N.; Ohki, Y.; Tanaka, T.; Imai, T.; Harada, M.; Ochi, M. *IEEE Trans Dielectr Electr Insul* 2008, 15, 24.
10. Harada, M.; Aoki, M.; Ochi, M. *J Network Polym Jpn* 2008, 29, 38.
11. Konda, T.; Yoshimura, T.; Saito, E.; Hayashi, T.; Miwa, K. *J Network Polym Jpn* 2003, 24, 186.
12. Mohan, T. P.; Kumar, M. R.; Velmurugan, R. *J Mater Sci* 2006, 41, 5915.
13. Jin, F.-L.; Han, M.; Park, S.-J. *Polym Int* 2006, 55, 1289.
14. Chen, B.; Liu, J.; Chen, H.; Wu, J. *Chem Mater* 2004, 16, 4864.
15. Okumura, H.; Takeoka, Y.; Hasegawa, K.; Kadota, J. *J Network Polym Jpn* 2004, 25, 131.
16. Brown, J. M.; Curliss, D.; Vaia, R. A. *Chem Mater* 2000, 12, 3376.
17. Mittal, V. *J Mater Sci* 2008, 43, 4972.
18. Miyagawa, H.; Drzal, L. T. *J Adhesion Sci Technol* 2004, 18, 1571.
19. Seo, K. S.; Kim, D. S. *Polym Eng Sci* 2006, 46, 1318.
20. Ratna, D.; Chakraborty, B. C.; Dutta, H.; Banthia, A. K. *Polym Eng Sci* 2006, 46, 1667.
21. Kornmann, X.; Thomann, R.; Muelhaupt, R.; Finter, J.; Berglund, L. *J Appl Polym Sci* 2002, 86, 2643.
22. Kornmann, X.; Thomann, R.; Muelhaupt, R.; Finter, J.; Berglund, L. *Polym Eng Sci* 2002, 42, 1815.
23. Kornmann, X.; Lindberg, H.; Berglund, L. A. *Polymer* 2001, 42, 4493.
24. Schartel, B.; Knoll, U.; Hartwig, A.; Pütz, D. *Polym Adv Technol* 2006, 17, 281.
25. Lakshmi, M. S.; Narmadha, B.; Reddy, B. S. R. *Polym Degrad Stab* 2008, 93, 201.
26. Saitoh, K.; Ohashi, K.; Hasegawa, K.; Kadota, J.; Hirano, H. *J Network Polym Jpn* 2009, 30, 69.